Structure, Vol. 12, 1719–1728, September, 2004, ©2004 Elsevier Ltd. All rights reserved. DOI 10.1016/j.str.2004.07.012

The CAP-Gly Domain of CYLD Associates with the Proline-Rich Sequence in NEMO/IKKγ

Kohei Saito,[1] Takanori Kigawa,[1] Seizo Koshiba,[1] Kazuo Sato,[1,2] Yo Matsuo,[1,2] Ayako Sakamoto,[1] Tetsuo Takagi,[1] Mikako Shirouzu,[1,3] Takashi Yabuki,[1] Emi Nunokawa,[1] Eiko Seki,[1] Takayoshi Matsuda,[1] Masaaki Aoki,[1] Yukako Miyata,[1] Noriko Hirakawa,[1] Makoto Inoue,[1] Takaho Terada,[1,3] Takahiro Nagase,[4] Reiko Kikuno,[4] Manabu Nakayama,[4] Osamu Ohara,[4,5] Akiko Tanaka,[1] and Shigeyuki Yokoyama[1,3,6,*]

[1]RIKEN Genomic Sciences Center
1-7-22 Suehiro-cho
Tsurumi, Yokohama 230-0045
Japan

[2]Graduate School of Integrated Science
Yokohama City University
1-7-26 Suehiro-cho
Tsurumi, Yokohama 230-0045
Japan

[3]RIKEN Harima Institute at SPring-8
1-1-1 Kouto
Mikazuki-cho, Sayo, Hyogo 679-5148
Japan

[4]Facility for Genome Structure Analysis
Kazusa DNA Research Institute
2-6-7 Kazusakamatari
Kisarazu, Chiba 292-0818
Japan

[5]RIKEN Research Center for Allergy and Immunology
1-7-22 Suehiro-cho
Tsurumi, Yokohama 230-0045
Japan

[6]Department of Biophysics and Biochemistry
Graduate School of Science
The University of Tokyo
7-3-1 Hongo
Bunkyo-ku, Tokyo 110-0033
Japan

Summary

CYLD was originally identified as the human familial cylindromatosis tumor suppressor. Recently, it was reported that CYLD directly interacts with NEMO/IKKγ and TRAF2 in the NF-κB signaling pathway. The two proteins bind to a region of CYLD that contains a Cys-box motif and the third cytoskeleton-associated protein-glycine conserved (CAP-Gly) domain. Here we report that the third CAP-Gly domain of CYLD specifically interacts with one of the two proline-rich sequences of NEMO/IKKγ. The tertiary structure of the CAP-Gly domain shares the five-stranded β sheet topology with the SH3 domain, which is well known as a proline-rich sequence-recognition domain. However, chemical shift mapping revealed that the peptide binding site of the CAP-Gly domain is formed without the long peptide binding loop characteristic of the SH3 domain. Therefore, CAP-Gly is likely to be a novel proline-rich sequence binding domain with a mechanism different from that of the SH3 domain.

*Correspondence: yokoyama@biochem.s.u-tokyo.ac.jp

Introduction

Familial cylindromatosis (turban tumor syndrome) is an autosomal dominant predisposition to multiple neoplasms of the skin appendages. The tumors, called cylindromas because of their characteristic microscopic architecture, arise mainly in hairy areas of the body, especially on the head and neck. The gene responsible for the disease (*cyld*) is located on chromosome 16q12-13 (Biggs et al., 1995, 1996; Thomson et al., 1999; Takahashi et al., 2000). The *cyld* gene product (CYLD) comprises 956 amino acid residues and contains a ubiquitin carboxyl-terminal hydrolase (UCH) catalytic domain (Bignell et al., 2000) (Figure 1A). Recently, the participation of CYLD in the NF-κB signaling pathway was reported (Brummelkamp et al., 2003; Kovalenko et al., 2003; Trompouki et al., 2003).

NF-κB plays prominent roles in the inducible expression of genes involved in diverse biological processes, including development, immune and inflammatory responses, cell growth and death, stress responses, and oncogenesis (for review, see Ghosh and Karin, 2002). Cell stimulation with a variety of agonists triggers the signal pathways that ultimately result in the activation of IκB kinase (IKK). It appears that CYLD directly interacts with the carboxyl-terminal region of the NF-κB essential modulator (NEMO/IKKγ) and regulates the kinase activity of IKK through the deubiquitination of tumor necrosis factor (TNF) receptor-associated factors (TRAF). Six members of the TRAF family have been identified, and their proteins share a carboxyl terminal homology region termed the TRAF (or MATH) domain (Uren and Vaux, 1996). TRAF proteins act as cytoplasmic adaptors that directly interact with the intracellular domains of cell surface receptors (for review, see Arch et al., 1998; Bradley and Pober, 2001). The recognition of diverse receptors by TRAF was revealed by structural studies (Park et al., 1999; Ye et al., 1999; McWhirter et al., 1999; Ni et al., 2000). A TRAF2 consensus binding sequence exists within CYLD (457-PVQES-461), and the interaction is lost by mutating S461 of CYLD, indicating that the region is the TRAF2 binding site (Kovalenko et al., 2003). The NF-κB-inducing activity of TRAFs depends on their RING finger-dependent ubiquitin ligase activity and autoubiquitination (Wang et al., 2001; Shi and Kehrl, 2003). The autoubiquitination requires the activity of the ubiquitin-conjugating enzyme Ubc13, which facilitates polyubiquitination formation through K63, although this ubiquitination does not mediate degradation, in contrast to K48 polyubiquitination (Deng et al., 2000).

NEMO/IKKγ is a regulatory subunit of the IKK complex

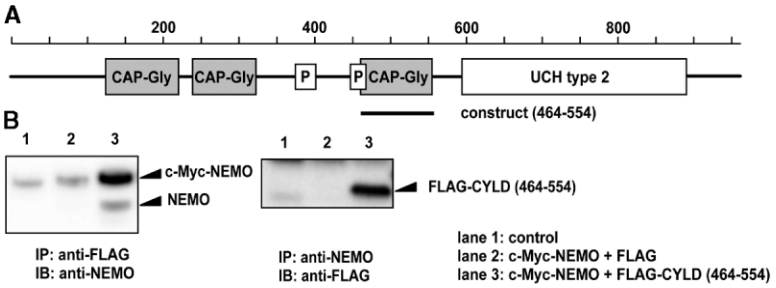

Figure 1. The Third CAP-Gly Domain in Human CYLD Protein Binds NEMO/IKKγ

(A) Domain structure of the human CYLD protein. CYLD contains three CAP-Gly domains, two proline-rich regions (indicated as P), and one ubiquitin carboxyl-terminal hydrolase type 2 catalytic domain (UCH type 2).

(B) NEMO/IKKγ and the third CAP-Gly domain of CYLD were coprecipitated in coexpressed cell extracts. FLAG-tagged CYLD constructs and c-Myc-tagged NEMO/IKKγ were coexpressed in HeLa cells. The extracts were immunoprecipitated (IP) with anti-Flag affinity gel (left) or anti-c-*myc* antibody (right) and immunoblotted (IB) with anti-NEMO/IKKγ (right) or anti-Flag (right) antibodies.

(Rothwarf et al., 1998; Yamaoka et al., 1998). NEMO/IKKγ contains several putative motifs: the amino-terminal large coiled-coil domain, which is required for binding to IKKβ, and the carboxyl-terminal domain, which comprises three subdomains including a coiled coil, a leucine zipper, and a zinc finger. Genetic studies suggested that NEMO/IKKγ is necessary for the activation of IKK within the NF-κB signaling pathway by diverse stimuli. The complete loss of NF-κB activity was shown by various stimuli in mouse knockout experiments (Rudolph et al., 2000; Makris et al., 2000; Schmidt-Supprian et al., 2000). Moreover, two types of human disorders have been genetically linked to mutations in the NEMO/IKKγ gene. Nonsense mutations in the NEMO/IKKγ gene are associated with incontinentia pigmenti (Smahi et al., 2000), whereas point mutations in the encoded carboxyl-terminal zinc finger domain, affecting only a subset of NF-κB activation pathways, are found in patients with anhidrotic ectodermal dysplasia in conjugation with immunodeficiency syndromes (Doffinger et al., 2001; Jain et al., 2001). TNF-α stimulates the K6-linked ubiquitination of NEMO/IKKγ, which is mediated by c-IAP1, an inhibitor of apoptosis protein (Tang et al., 2003). On the other hand, B cell lymphoma/leukemia 10 (Bcl10) targets NEMO/IKKγ for K63-linked ubiquitination at K399, which is located in the carboxyl-terminal zinc finger of NEMO/IKKγ (Zhou et al., 2004). NEMO/IKKγ is also modified by the small ubiquitin-like modifier (SUMO), and its subsequent ubiquitination mediates NF-κB activation by relocalizing NEMO/IKKγ from the nucleus to the cytoplasm (Huang et al., 2003).

CYLD contains three CAP-Gly domains in its amino terminus (Bignell et al., 2000). The CAP-Gly domain consists of about 70 amino acid residues, with the characteristically conserved hydrophobic and glycine residues. This domain exists in several microtubule (MT) binding proteins, such as the cytoplasmic linker protein CLIP-170 (Restin), p150glued (Dynactin 1), and the tubulin folding cofactors B and E (Riehemann and Sorg, 1993). It appears that the domains themselves are responsible for their colocalization with MT (Pierre et al., 1994; Feierbach et al., 1999; Scheel et al., 1999; Radcliffe and Toda., 2000). Although it is not known whether CYLD colocalizes with MT and whether the CAP-Gly domains of CYLD can bind to MT, we considered that the domains could be responsible for protein-protein interactions, including MT binding. In this study, we have determined the three-dimensional structure of the third CAP-Gly domain of CYLD by NMR spectroscopy. Based on chemical shift perturbation data, we provide evidence that the CAP-Gly domain specifically interacts with one of the two proline-rich sequences of NEMO/IKKγ.

Results

The Third CAP-Gly Domain Is Needed for NEMO/IKKγ Binding

NEMO/IKKγ binds to the region encompassing residues 470–684 in CYLD (Kovalenko et al., 2003), which contains the third CAP-Gly domain and the Cys-box motif. Structurally, the Cys-box belongs to the UCH catalytic domain (Hu et al., 2002), and therefore we thought that the CAP-Gly domain might be a NEMO/IKKγ binding site. In order to evaluate this hypothesis, the construct (residues 464–554) containing only the CAP-Gly domain was coexpressed with full-length NEMO/IKKγ in cultured cells, and their extracts were coimmunoprecipitated (Figure 1B). The CAP-Gly domain was coprecipitated with NEMO/IKKγ and vice versa. Moreover,

Table 1. Structural Statistics for the CAP-Gly Domain—20 Structures

NOE distance constraints	
Intraresidue	839
Sequential	585
Medium-range	333
Long-range	910
Dihedral angle constraints	
Main chain (ϕ/ψ)	90
Side chain (χ_1)	30
Root-mean-square deviation from idealized covalent geometry	
Bonds (Å)	0.0006 ± 0.00005
Angles (°)	0.251 ± 0.0012
Impropers (°)	0.085 ± 0.0012
Root-mean-square deviation from experimental restraints	
NOE (Å)	0.0014 ± 0.0005
Dihedrals (°)	0.13 ± 0.012
Ramachandran plot (%)	
Most favored region	74.1
Additionally allowed region	25.5
Generously allowed region	0.1
Disallowed region	0.3
Root-mean-square deviation to the mean structure (Å)	
Backbone (residues 473–548)	0.40 ± 0.06
Nonhydrogen atoms (residues 473–548)	0.90 ± 0.08

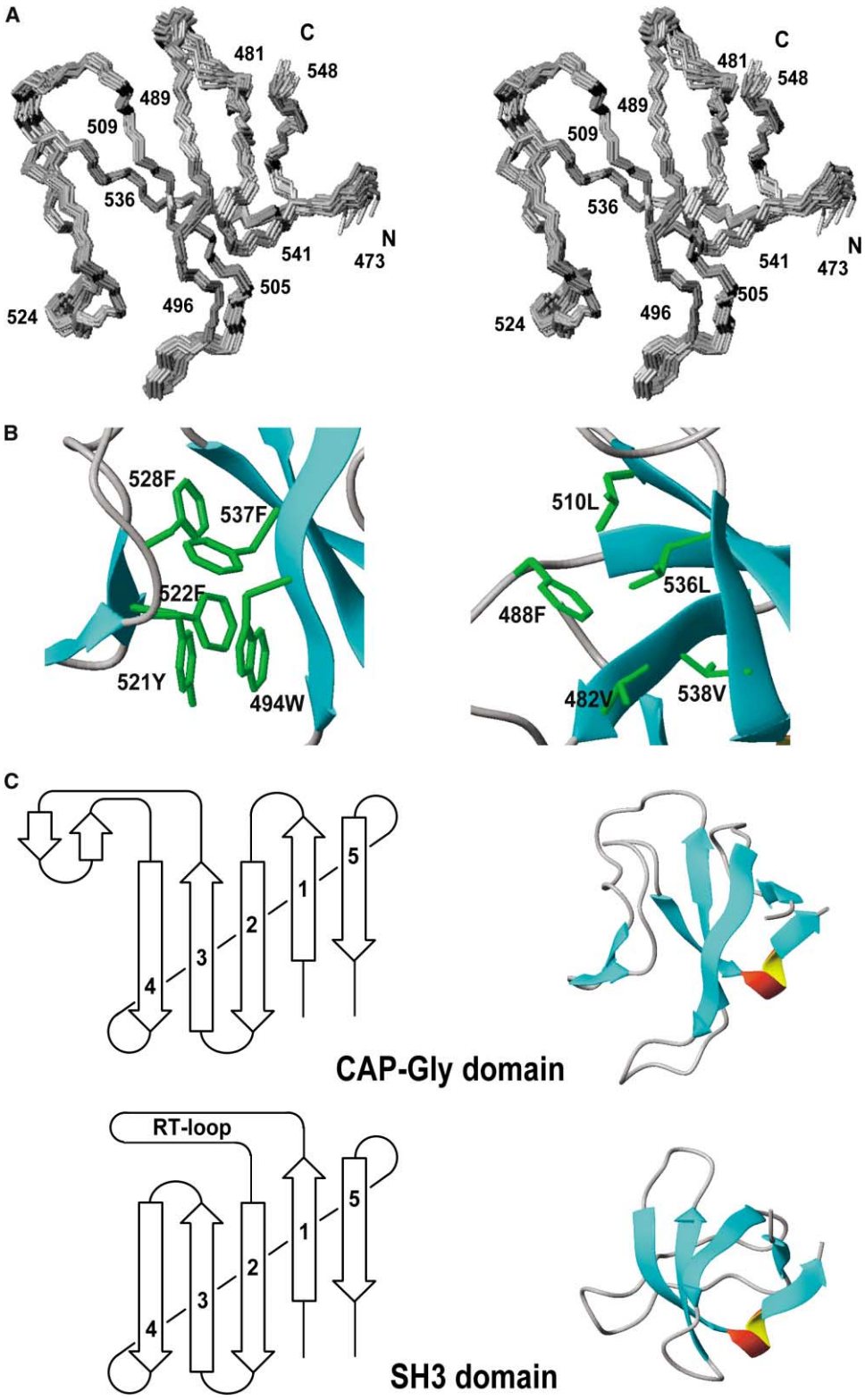

Figure 2. The CAP-Gly Domain Structure

(A) Best-fit superpositions of the final 20 simulated annealing structures of the CAP-Gly domain. Only the main chains of residues 473–548 are presented.

(B) Two major hydrophobic cores. Hydrophobic and aromatic side chains are presented in green.

(C) The structures (represented by ribbon models and topology diagrams) of the CAP-Gly and the SH3 domain of c-CRK (PDB code: 1CKA) are compared. The five common β strands are numbered.

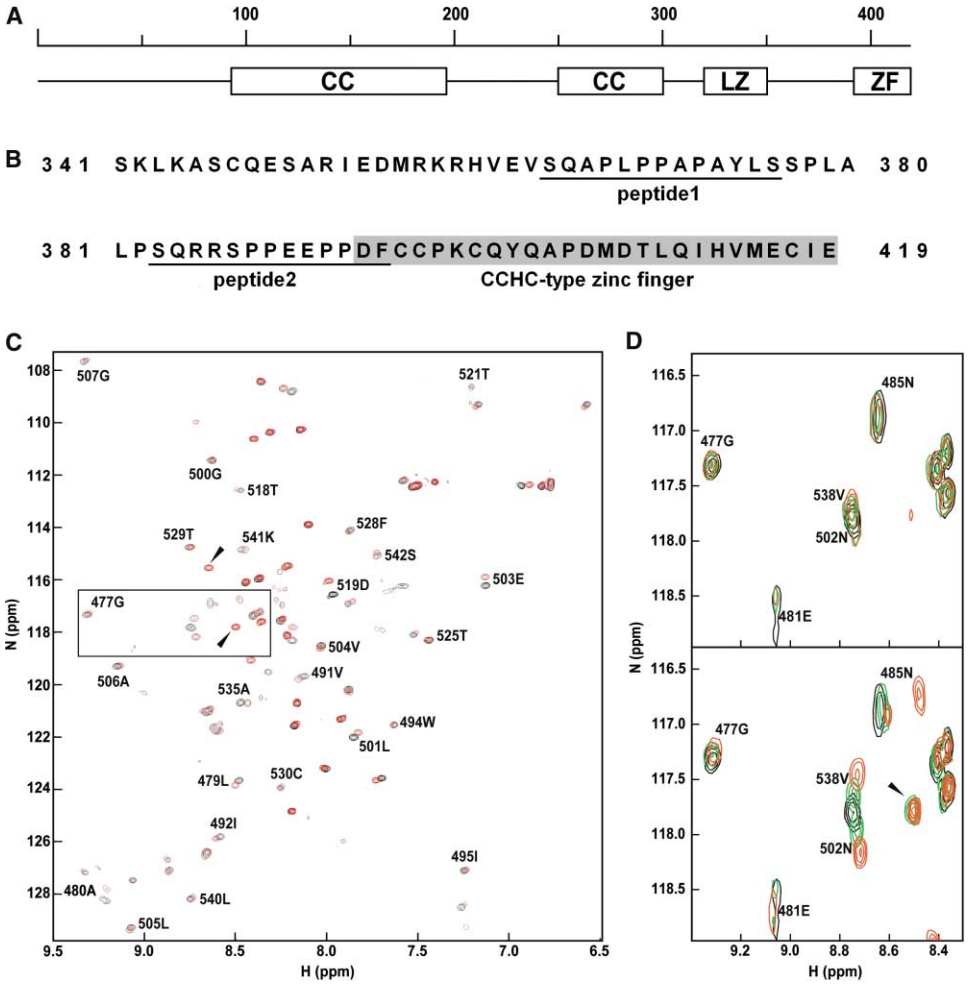

Figure 3. The CAP-Gly Domain Specifically Interacts with One of the Two Proline-Rich Sequences of NEMO/IKKγ

(A) Domain structure of NEMO/IKKγ. The coiled-coil (CC), leucine-zipper (LZ), and zinc finger (ZF) motifs are presented.

(B) Primary sequence of the carboxyl terminus of human NEMO/IKKγ. The CCHC-type zinc finger motif is shaded, and the two peptide sequences used for the perturbation study are underlined.

(C) Comparison of the ^{1}H, ^{15}N correlation spectra of the CAP-Gly domain in the absence (black) and presence of 10 (red) molar equivalents of peptide2. The crosspeaks that appeared upon peptide addition are indicated by arrowheads. The boxed region is magnified and presented in (D).

(D) Detailed comparison of the ^{1}H, ^{15}N correlation spectra of the CAP-Gly domain in the absence (black) and presence of 5 (green) or 10 (red) molar equivalents of peptide1 (upper panel) or peptide2 (lower panel).

endogenous NEMO was coprecipitated with the CAP-Gly domain (Figure 1B, left panel, lanes 3), strengthening the idea that the CAP-Gly domain contains the structural elements needed for NEMO/IKKγ binding.

The Solution Structure of the CAP-Gly Domain

The solution structure of the third CAP-Gly domain was calculated (Table 1). The structure of residues 473–548 is well defined (Figure 2A) and consists of a five-stranded (residues 479–481, 489–496, 505–509, 536–539, and 543–545) antiparallel β sheet with an inserted antiparallel β sheet-like loop (residues 511–534). There are two significant hydrophobic cores in the domain. One consists of five aromatic side chains (W494, Y521, F522, F528, and F537) between the β sheet and the β sheet-like loop (Figure 2B, left). The other consists of V482, F488, L510, L536, and V538, which make a barrel-like fold (Figure 2B, right).

The crystal structure of the CAP-Gly domain from nematode hypothetical protein was reported (Li et al., 2002), and its folding topology is quite similar. One significant difference is the existence of an additional α helix within the amino-terminal region. No significant nonsequential interresidue NOEs were observed in this region when the longer construct was analyzed (residues 414–558; data not shown), indicating that it is unstructured.

The folding topology of the CAP-Gly domain resembles that of the src homology 3 (SH3) domain (Figure 2C). The two proteins share similar topologies of the five β strands. The SH3 domain is well known as a proline-rich peptide binding motif, and its RT loop is involved in ligand recognition (for review, see Macias et

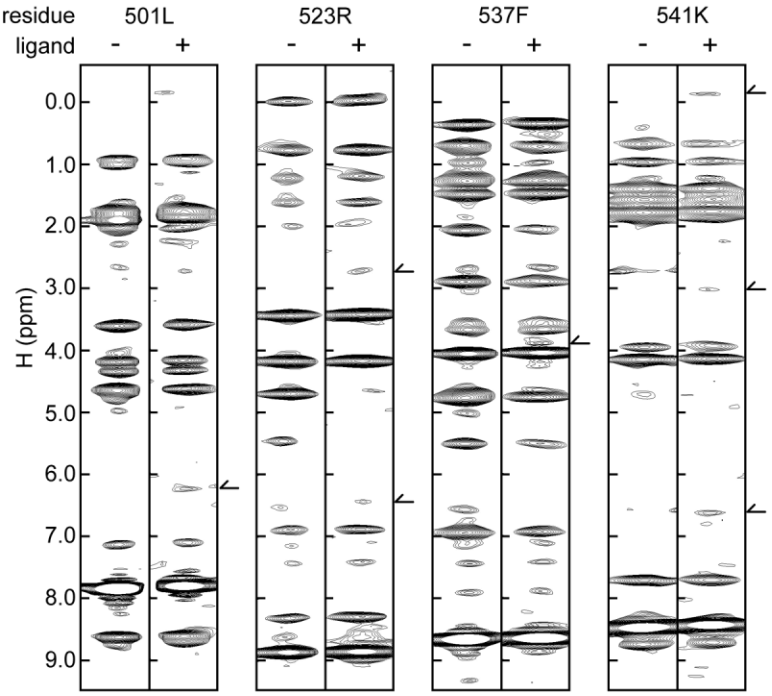

Figure 4. The ^{15}N-NOESY Spectra of the Representative Amide Protons

The NOE crosspeaks were compared in the absence (left) and presence (right) of the ligand. The peaks that appeared upon ligand addition are indicated by arrows.

al., 2002). Although the inserted positions of the long loops in the primary sequence are distinct between the SH3 and CAP-Gly domains, they are close in the tertiary structure. In addition, the shape of the ligand binding surface in the SH3 domain is somewhat similar to the corresponding surface in the CAP-Gly domain. Thus, the CAP-Gly domain may also interact with a proline-rich ligand.

The CAP-Gly Domain Interacts with One of the Two Proline-Rich Sequences of NEMO/IKKγ

The carboxyl-terminal 39 amino acid residues in NEMO/IKKγ interact with CYLD (Kovalenko et al., 2003). This region contains a CCHC-type zinc finger motif and a flanking proline-rich sequence (388-PPEEPP-393) (Figures 3A and 3B). Thus, we expected that the CAP-Gly domain could recognize the sequence. In addition, we found another proline-rich sequence just before the region (369-PPAP-372). In order to assess the interactions between the CAP-Gly domain and these putative binding sites with atomic detail, heteronuclear correlation experiments were carried out, and the ^{1}H and ^{15}N chemical shift changes were monitored upon the addition of the peptides (Figure 3C). The CAP-Gly domain spectra were not affected by the addition of the peptide containing 369-PPAP-372, even at peptide to protein molar ratios as high as 10 (Figure 3D, upper panel). In contrast, several crosspeaks changed when the peptide containing 388-PPEEPP-393 was added to the protein (Figures 3C and 3D, lower panel). Particularly, the amide crosspeaks of N502 and V538 gradually shifted with the amount of added peptide, indicating that the exchange between the free- and bound forms is fast on the NMR time scale. Interestingly, the movement of the N485 peak shows a slow exchange mode. In the absence of the peptide, the crosspeak of E481 was broad, and furthermore, the crosspeaks of V482, K483, and E484, which are the turn conformation between β strands 1 and 2, were too broad to be observed (assuming exchange broadening). Actually, the numbers of NOEs are smaller than those of other residues, and therefore the turn region is relatively not well ordered (Figure 2A). However, the peak of E481 gradually became sharper, and unassigned peaks (indicated by arrowheads in Figures 3C and 3D) appeared with the addition of the peptide. These findings suggested that the conformation of the turn is originally multiple but becomes more restricted upon ligand binding. Similar phenomena were observed by decreasing the temperature of the ligand-free sample (data not shown), which was also expected to reduce the conformation exchange rate of the turn. A comparison of the ^{15}N-NOESY spectra in the presence and absence of the peptide (Figure 4) revealed several new peaks, which appeared upon peptide addition.

Ten human proteins, with a total of 17 CAP-Gly domains, have been found (Figure 5A). The residues conserved in the human CAP-Gly domains and those showing alterations, such as shifting, disappearing, sharpening, or broadening, during the perturbation study were compared (Figures 5B–5D). One highly conserved surface (right panels in Figures 5B–5D) is obviously not involved in the interaction with the proline-rich peptide. In contrast, the concave surface, which corresponds to the proline-rich peptide binding surface, also shows conservation. The surface forms a hydrophobic cleft consisting of several hydrophobic residues, such as L505, L510, F522, L536, F537, and V538. This hydrophobic environment may be a key feature of the proline-rich sequence recognition, and its conservation among the CAP-Gly domains suggests that this interaction is common among the CAP-Gly domains.

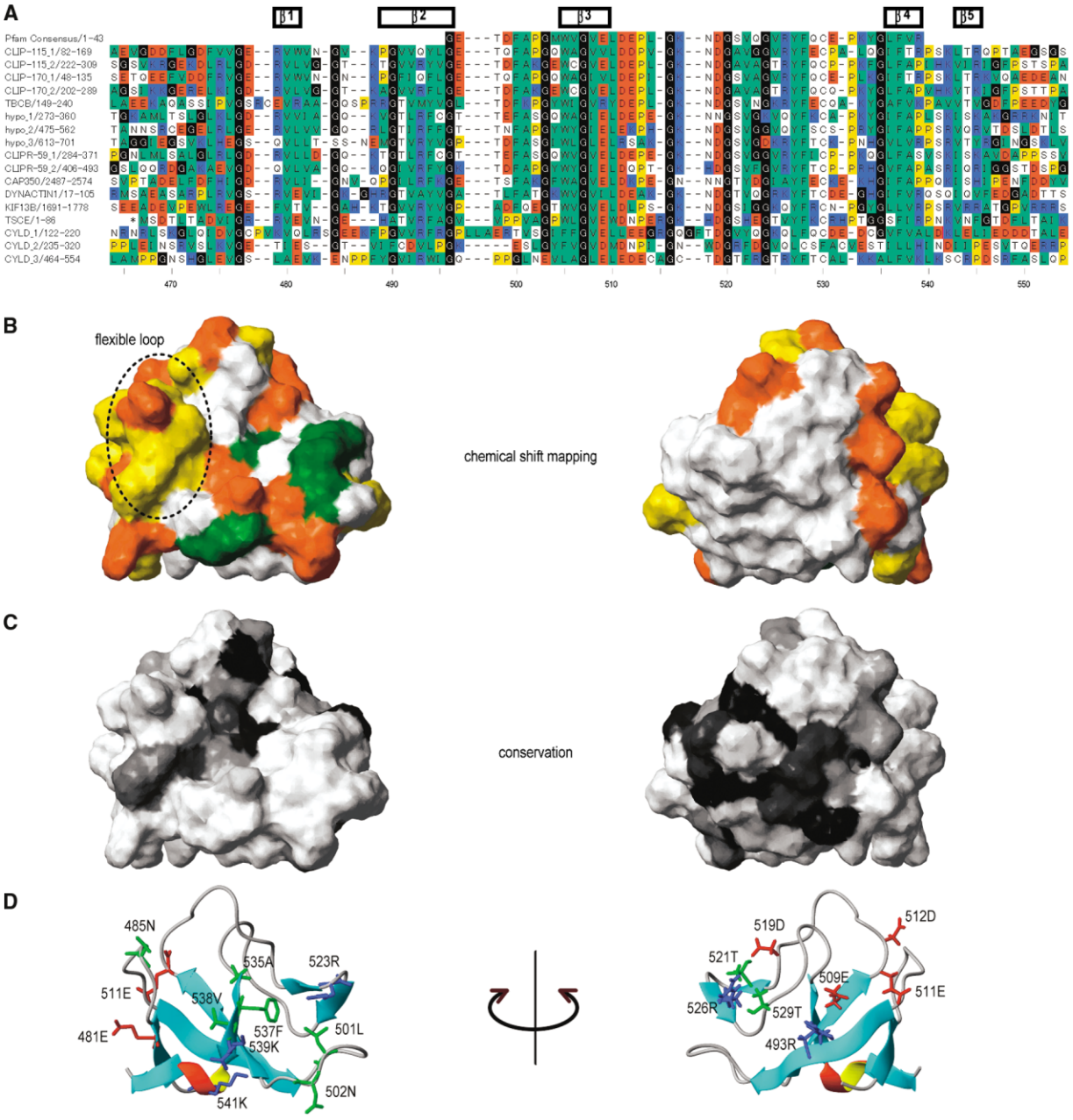

Figure 5. Mapping of the Ligand Binding and Conserved Surfaces on the CAP-Gly Domain

(A) Primary sequence alignment of human CAP-Gly domain-containing proteins. The sequences are CLIP-115 (NCBI Protein Database accession number BAA22960), CLIP-170 (P30622), TBCB (tubulin folding cofactor B, Q99426), hypo (hypothetical protein, NP_078968), CLIPR-59 (CLIP-170-related protein, NP_056341), CAP350 (centrosome-associated protein 350, NP_055625), DYNACTIN1 (Q14203), KIF13B (kinesin-like protein GAKIN, Q9NQT8), TSCE (*Homo sapiens* tubulin-specific chaperone E, AAP36804), and CYLD (BAA74872). Hydrophobic and aromatic (L, I, M, V, A, F, W, and Y), basic (K, R, and H), acidic (D and E), proline, and glycine residues are colored differently.

(B) Comparison of the chemical shift mapping results and the conserved residues on the CAP-Gly domains. Perturbed residues are colored orange, whereas residues that were not observed in the absence of any peptide are yellow. The residues indicated in Figure 4 are colored in green.

(C) Residue conservation is colored from black (highly conserved) to white (less conserved), as calculated from the sequence alignment of (A). The putative ligand binding surface shows conservation in the bottom of the hydrophobic cleft (left panel), and the highly conserved surface is observed on the other side (right panel).

(D) The residues mentioned in (B) and (C) are presented on ribbon models.

Discussion

The third CAP-Gly domain of CYLD lacks an α helix in its amino terminus (Figure 2), in contrast to the crystal structure of the CAP-Gly domain from nematode hypothetical protein (Li et al., 2002). The region was identified as a putative TRAF2 binding site in CYLD (457-PVQES-461 [Kovalenko et al., 2003]). The TRAF domain recog-

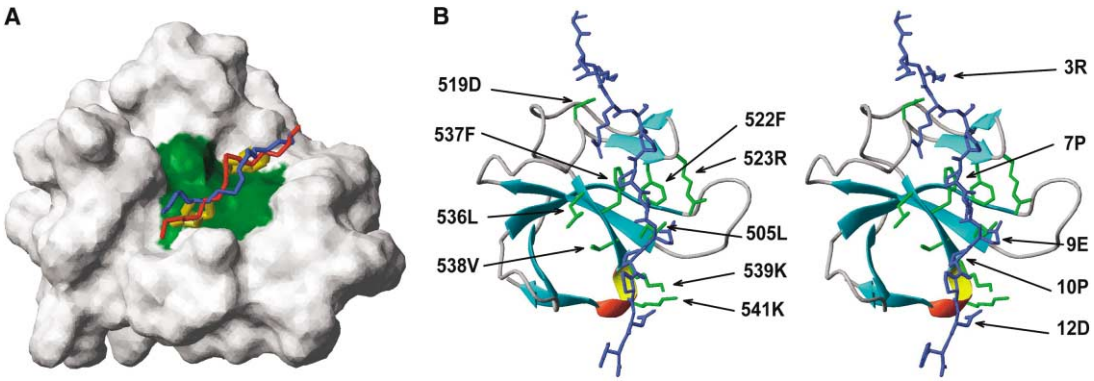

Figure 6. The Peptide-Bound Models of the CAP-Gly Domain

(A) The hydrophobic cleft in CAP-Gly, which is formed by L505, F522, L536, F537, and V538, is colored green. Two typical models that docked the peptide well in the hydrophobic cleft are presented. The backbones of the two peptides are colored in red and blue, respectively. Two of the proline side chains, corresponding to P7 and P10 in the SQRRSPPEEPPDF sequence, are colored yellow.

(B) Stereoview of the 13-mer peptide-bound model of the CAP-Gly domain. The residues that were expected to be involved in peptide recognition are presented in green and are labeled on the left. The residues of the peptide are labeled on the right.

nizes the extended structures of diverse receptors (Park et al., 1999; Ye et al., 1999; McWhirter et al., 1999; Ni et al., 2000), and therefore it is feasible that the putative TRAF binding site in CYLD is unstructured. The amino acid sequences of the amino-terminal regions in the CAP-Gly domains are not conserved at all (Figure 5A), and therefore the presence/absence of an α helix there seems to be one variation in the CAP-Gly family.

The fold of the CAP-Gly domain resembles that of the SH3 domain (Figure 2), and the CAP-Gly domain binds to the proline-rich sequence of NEMO/IKKγ (Figure 3). The SH3 domain, as well as the WW, GYF, and EVH1 domains, is known as a proline-rich ligand binding motif, and the conserved aromatic residues in the respective fold families constitute a major interaction site for the proline residues of the ligand (Prehoda et al., 1999; Freund et al., 2002; Macias et al., 2002). Although L505 of the third CAP-Gly domain of CYLD is not an aromatic residue, the corresponding residue is conserved as an aromatic residue among the rest of the proteins in the family. The position of Y527 is highly conserved as tyrosine, except for the first and the second CAP-Gly domains of CYLD, and F537 is also conserved in the family (Figure 5A). Interestingly, these residues are exposed on the putative ligand binding surface.

Ligand binding to the CAP-Gly domain may not occur in a simple two-state binding mode, because both slow and fast modes were observed in the perturbation study (Figure 3D). One reason is that the mobile turn between β strands 1 and 2 may contribute to the interaction. Interestingly, the primary sequence of the turn corresponds to that of the RT loop in SH3; however, these regions seem to have different roles in their ligand recognition. The amino acid sequences of the turn region are variable in the CAP-Gly family (Figure 5A), suggesting that this complex binding mode is not a general feature among the CAP-Gly family members.

Two PPEEPP hexapeptide bound models of the CAP-Gly domain are proposed in Figure 6. These peptides are positioned in opposite directions, but two proline residues (colored yellow in Figure 6A) have quite similar locations. Especially, one proline side chain (proline 7 in Figure 6B) seems to interact with the aromatic side chains of F522 and F537 (Figure 6B). This kind of interaction is often observed in ligand proline recognition in many proline-rich sequence recognition domains (Macias et al., 2002; Freund et al., 2002). The direction of the ligand peptide is known to be determined, not by the PxxP sequence, but by the flanking charged residue in the case of the SH3 domain (Cesareni et al., 2002).

Although there were only a few NOESY crosspeaks and we could not assign them exactly (Figure 4), we can speculate on the ligand binding by their chemical shift values and the complex model presented in Figure 6. For example, the amide proton of F537 is located at the bottom of the hydrophobic cleft, so the new peak around 3.8 ppm is probably derived from the δ proton of one of the proline residues in the ligand (Figure 6B). There is no aromatic side chain around the amide proton of K541, but new peaks appeared around -0.1 and 6.7 ppm. These peaks indicate that the phenylalanine side chain in the ligand resides around the amide proton (Figure 6B), because the chemical shift value of 6.7 ppm is in good agreement with the δ, ϵ, or ζ proton of a phenylalanine residue, and a chemical shift value of -0.1 ppm is usually observed when a proton stacks against an aromatic side chain. If these speculations are actually the case, then these NOEs support the suggestion that the peptide direction from left to right in Figure 6A is more likely than the opposite configuration.

Notably, the interaction between the CAP-Gly domain and the proline-rich peptide seemed to be weak, because a 10-fold molar excess of the peptide to the protein was required for saturation (the dissociation constant was estimated at 10^{-4}–10^{-3} M by the NMR titration study). It is true that signaling interactions are often intrinsically weak, but we should mention a few possibilities for this weak interaction. We used synthetic, 13 amino acid length peptides in this study. There are several reports that a neighboring structural motif also contributes to the interaction by the SH3 and WW domains (Huang et al., 2000; Ghose et al., 2001; Kami et al., 2002). The zinc finger motif is flanked by the proline-rich sequence of NEMO/IKKγ, while there are two more

CAP-Gly domains in CYLD. In cells, CYLD reportedly interacts with both NEMO/IKKγ and TRAF (Brummelkamp et al., 2003; Kovalenko et al., 2003; Trompouki et al., 2003); however, it is unlikely that only CYLD links NEMO/IKKγ to TRAF. Furthermore, regulation by post-translational modifications, such as phosphorylation and ubiquitination, should be considered. The carboxyl-terminal region of NEMO/IKKγ is required for IKK activation (Huang et al., 2002; Makris et al., 2002), and this region may recruit IKK to the upstream signaling components or may regulate specific NEMO modifications to permit IKK activation (Huang et al., 2003).

Most of the CAP-Gly domain-containing proteins are considered as cytoskeleton-associated proteins, and the domains themselves are responsible for MT binding (Pierre et al., 1994; Feierbach et al., 1999; Scheel et al., 1999; Radcliffe and Toda, 2000). In the yeast CAP-Gly domain of Alf1p, the homolog of mammalian tubulin folding cofactor B, a triple mutation (GKNDG to AENDA, corresponding to G516, C517, and G520 in human CYLD) disrupts the interaction with α-tubulin (Feierbach et al., 1999). These residues are involved in our putative ligand binding surface, and the residue at 517 in CYLD is cysteine, in spite of its high conservation as a lysine residue in the CAP-Gly domain family (Figure 5A). The amino acid sequences of the CAP-Gly domains in CYLD are relatively less conserved among the CAP-Gly domains. If the basic side chain contributes significantly to MT binding, then CYLD may not interact with microtubules; however, β-tubulin, as well as Cdc37 and Hsp90, reportedly exists in the IKK complex (Chen et al., 2002).

From this study, we conclude that the CAP-Gly domain of CYLD associates with the proline-rich sequence of NEMO/IKKγ. Indeed, the CAP-Gly domain is probably a proline-rich ligand binding motif.

Experimental Procedures

Immunoprecipitation

HeLa cells were transfected with c-*myc*-tagged human NEMO/IKKγ and Flag-tagged human CYLD (KIAA0849 [Kikuno et al., 2002]) expression vectors. After 24 hr, the cells were lysed in buffer (30 mM Tris-HCl [pH 7.4], 150 mM NaCl, 5 mM EDTA, and 1% Triton-X100). Cleared cell extracts were incubated with 10 μg of anti-Flag M2 Affinity Gel (Sigma) and 30 μg of protein G (SIGMA). For precipitating NEMO/IKKγ, an anti-c-*myc* antibody was used.

Sample Preparation

The CAP-Gly construct of human CYLD was cloned into the expression vector pCR2.1 (Invitrogen) as a fusion with an amino-terminal 6-His affinity tag and a TEV protease cleavage site. The fusion protein was synthesized by a cell-free protein expression system (Kigawa et al., 1999, 2004). The protein was first adsorbed to a HiTrap Chelating HP column (Amersham), which was washed with a concentration gradient of buffer (50 mM sodium phosphate [pH 8.0] containing 0.5 M sodium chloride and 10 mM imidazole). The protein was eluted with a concentration gradient of imidazole (from 10 to 500 mM). The His-tag was then removed by an incubation at 30°C for 1 hr with the TEV protease. The construct 464–554, which was used for structure determination, contains the artificial sequences GSSGSSG and SGPSSG at the amino- and carboxyl termini, respectively. The imidazole and sodium phosphate were removed by an overnight dialysis at 4°C against 50 mM sodium phosphate buffer (pH 8.0) containing 1 mM DTT. Finally, the protein was purified on a HiTrap Q HP column (Amersham) by a concentration gradient of 0–1 M sodium chloride. For NMR measurements, this purified protein was concentrated up to ~1.0 mM in H_2O/D_2O (9:1) 20 mM sodium phosphate buffer (pH 6.0) containing 100 mM sodium chloride and 1 mM DTT.

NMR Spectroscopy

All NMR spectra were acquired at 25 C° on 600 and 800 MHz Bruker Avance NMR spectrometers. The backbone and side chain ^{1}H, ^{13}C, and ^{15}N resonances of the protein were assigned using the triple resonance spectra of HNCA, HN(CO)CA, HNCACB, CBCA(CO)NH, C(CO)NH-TOCSY HBHA(CO)NH, (H)C(CO)NH-TOCSY, 3D HCCH-TOCSY, and 3D HCCH-COSY (Clore and Gronenborn, 1994), recorded on a uniformly $^{15}N/^{13}C$-labeled protein. NOE-derived distance constraints were obtained from ^{15}N- or ^{13}C-edited 3D NOESY spectra.

For chemical shift mapping studies, 0.3 mM ^{15}N-labeled construct was used. ^{1}H, ^{15}N correlation spectra were measured in the absence and presence of peptides derived from the human NEMO/IKKγ sequence (peptide1: SQAPLPPAPAYLS; peptide2: SQRRSPPEEPPDF) up to a molar ratio of 1:10.

Distance Constraints and Structure Calculations

Interproton distance restraints were obtained from NOESY spectra, with a mixing time of 80 ms. NOE data were translated to upper limit distance restraints based on -6 order formulas of the intensity and the distance. Lower distance bounds were set to 1.8 Å. The secondary structured regions were determined by manually assigning the interproton NOE peaks, and the ϕ/ψ angular constraints were determined using the program TALOS (Cornilescu et al., 1999) with a $\pm 30°$ range. Additionally, the side chain angular constraints of χ_1 were determined by a combination of the peak patterns in HNCOHB and HNHB experiments (Powers et al., 1993).

Structures were calculated using a mixed torsion and Cartesian angle dynamics simulated annealing protocol with the program CNS (Brunger et al., 1998) version 1.1. The starting structure was generated as an extended form, and all force constants and molecular parameters were set to their default values, with the exception of the number of steps, which was increased to 4000 steps for the high-temperature annealing stage, 4000 steps for the first slow-cool annealing stage, and 6000 steps for the second slow-cool annealing stage. Structure modeling, visualization, and superimposition were done using MOLMOL (Koradi et al., 1996).

Model Building

The initial structure of the Ace-PPEEPP-NMe hexapeptide was constructed by homology modeling using the 86-FPEEPP-91 region of PDB code 1A21. The docking simulation was carried out by AutoDock version 3.0.5 (Morris et al., 1998) with fixing of the ϕ and ψ angles of the peptide. The search region on the CAP-Gly domain was restricted to one side involving the hydrophobic cleft presented in Figure 6. Initially, 100 models were outputted, and 11 models were selected by the final docked energy (less than -5 kcal/mol) and the structural dissimilarity (more than 3 Å root-mean-square-deviations against the others). The SQRRSPPEEPPDF peptide model was created based on the most feasible PPEEPP model, which was selected manually, and the energy was minimized.

Acknowledgments

The authors thank Y. Fujikura, N. Matsuda, Y. Motoda, M. Saito, A. Kobayashi, N. Sakagami, M. Ikari, F. Hiroyasu, Y. Tomo, and S. Yasuda for help with sample preparations and maintaining the NMR facility. This work was supported by the RIKEN Structural Genomics/Proteomics Initiative (RSGI), the National Project on Protein Structural and Functional Analyses, Ministry of Education, Culture, Sports, Science and Technology of Japan.

Received: March 16, 2004
Revised: July 1, 2004
Accepted: July 6, 2004
Published: September 7, 2004

References

Arch, R.H., Gedrich, R.W., and Thompson, C.B. (1998). Tumor necrosis factor receptor-associated factors (TRAFs)—a family of adapter proteins that regulates life and death. Genes Dev. *12*, 2821–2830.

Biggs, P.J., Wooster, R., Ford, D., Chapman, P., Mangion, J., Quirk, Y., Easton, D.F., Burn, J., and Stratton, M.R. (1995). Familial cylindromatosis (turban tumour syndrome) gene localised to chromosome 16q12-q13: evidence for its role as a tumour suppressor gene. Nat. Genet. *11*, 441–443.

Biggs, P.J., Chapman, P., Lakhani, S.R., Burn, J., and Stratton, M.R. (1996). The cylindromatosis gene (cyld1) on chromosome 16q may be the only tumour suppressor gene involved in the development of cylindromas. Oncogene *12*, 1375–1377.

Bignell, G.R., Warren, W., Seal, S., Takahashi, M., Rapley, E., Barfoot, R., Green, H., Brown, C., Biggs, P.J., Lakhani, S.R., et al. (2000). Identification of the familial cylindromatosis tumour-suppressor gene. Nat. Genet. *25*, 160–165.

Bradley, J.R., and Pober, J.S. (2001). Tumor necrosis factor receptor-assoicated factors (TRAFs). Oncogene *20*, 6482–6491.

Brummelkamp, T.R., Nijman, S.M., Dirac, A.M., and Bernards, R. (2003). Loss of the cylindromatosis tumour suppressor inhibits apoptosis by activating NF-κB. Nature *424*, 797–801.

Brunger, A.T., Adams, P.D., Clore, G.M., DeLano, W.L., Gros, P., Grosse-Kunstleve, R.W., Jiang, J.S., Kuszewski, J., Nilges, M., Pannu, N.S., et al. (1998). Crystallography & NMR system: a new software suite for macromolecular structure determination. Acta Crystallogr. D Biol. Crystallogr. *54*, 905–921.

Cesareni, G., Panni, S., Nardelli, G., and Castagnoli, L. (2002). Can we infer peptide recognition specificity mediated by SH3 domains? FEBS Lett. *513*, 38–44.

Chen, G., Cao, P., and Goeddel, D.V. (2002). TNF-induced recruitment and activation of the IKK complex require Cdc37 and Hsp90. Mol. Cell *9*, 401–410.

Clore, G.M., and Gronenborn, A.M. (1994). Multidimensional heteronuclear nuclear magnetic resonance of proteins. Methods Enzymol. *239*, 349–363.

Cornilescu, G., Delaglio, F., and Bax, A. (1999). Protein backbone angle restraints from searching a database for chemical shift and sequence homology. J. Biomol. NMR *13*, 289–302.

Deng, L., Wang, C., Spencer, E., Yang, L., Braun, A., You, J., Slaughter, C., Pickart, C., and Chen, Z.J. (2000). Activation of the IkappaB kinase complex by TRAF6 requires a dimeric ubiquitin-conjugating enzyme complex and a unique polyubiquitin chain. Cell *103*, 351–361.

Doffinger, R., Smahi, A., Bessia, C., Geissmann, F., Feinberg, J., Durandy, A., Bodemer, C., Kenwrick, S., Dupuis-Girod, S., Blanche, S., et al. (2001). X-linked anhidrotic ectodermal dysplasia with immunodeficiency is caused by impaired NF-kappaB signaling. Nat. Genet. *27*, 277–285.

Feierbach, B., Nogales, E., Downing, K.H., and Stearns, T. (1999). Alf1p, a CLIP-170 domain-containing protein, is functionally and physically associated with α-tubulin. J. Cell Biol. *144*, 113–124.

Freund, C., Kuhne, R., Yang, H., Park, S., Reinherz, E.L., and Wagner, G. (2002). Dynamic interaction of CD2 with the GYF and the SH3 domain of compartmentalized effector molecules. EMBO J. *21*, 5986–5995.

Ghose, R., Shekhtman, A., Goger, M.J., Ji, H., and Cowburn, D. (2001). A novel, specific interaction involving the Csk SH3 domain and its natural ligand. Nat. Struct. Biol. *8*, 998–1004.

Ghosh, S., and Karin, M. (2002). Missing pieces in the NF-κB puzzle. Cell *109*, S81–S96.

Hu, M., Li, P., Li, M., Li, W., Yao, T., Wu, J.W., Gu, W., Cohen, R.E., and Shi, Y. (2002). Crystal structure of a UBP-family deubiquitinating enzyme in isolation and in complex with ubiquitin aldehyde. Cell *111*, 1041–1054.

Huang, X., Poy, F., Zhang, R., Joachimiak, A., Sudol, M., and Eck, M.J. (2000). Structure of a WW domain containing fragment of dystrophin in complex with beta-dystroglycan. Nat. Struct. Biol. *7*, 634–638.

Huang, T.T., Feinberg, S.L., Suryanarayanan, S., and Miyamoto, S. (2002). The zinc finger domain of NEMO is selectively required for NF-κB activation by UV radiation and topoisomerase inhibitors. Mol. Cell. Biol. *22*, 5813–5825.

Huang, T.T., Wuerzberger-Davis, S.M., Wu, Z.H., and Miyamoto, S. (2003). Sequential modification of NEMO/IKKgamma by SUMO-1 and ubiquitin mediates NF-kappaB activation by genotoxic stress. Cell *115*, 565–576.

Jain, A., Ma, C.A., Liu, S., Brown, M., Cohen, J., and Strober, W. (2001). Specific missense mutations in NEMO result in hyper-IgM syndrome with hypohydrotic ectodermal dysplasia. Nat. Immunol. *2*, 223–228.

Kami, K., Takeya, R., Sumimoto, H., and Kohda, D. (2002). Diverse recognition of non-PxxP peptide ligands by the SH3 domains from p67(phox), Grb2 and Pex13p. EMBO J. *21*, 4268–4276.

Kigawa, T., Yabuki, T., Yoshida, Y., Tsutsui, M., Ito, Y., Shibata, T., and Yokoyama, S. (1999). Cell-free production and stable-isotope labeling of milligram quantities of proteins. FEBS Lett. *442*, 15–19.

Kigawa, T., Yabuki, T., Matsuda, N., Matsuda, T., Nakajima, R., Tanaka, A., and Yokoyama, S. (2004). Preparation of Escherichia coli cell extract for highly productive cell-free protein expression. J. Struct. Funct. Genomics *5*, 63–68.

Kikuno, R., Nagase, T., Waki, M., and Ohara, O. (2002). HUGE: a database for human large proteins identified in the Kazusa cDNA sequencing project. Nucleic Acids Res. *30*, 166–168.

Koradi, R., Billeter, M., and Wuthrich, K. (1996). MOMOL: a program for display and analysis of macromolecular structures. J. Mol. Graph. *14*, 51–55.

Kovalenko, A., Chable-Bessia, C., Cantarella, G., Israel, A., Wallach, D., and Courtois, G. (2003). The tumour suppressor CYLD negatively regulates NF-κB signalling by deubiquitination. Nature *424*, 801–805.

Li, S., Finley, J., Liu, Z.J., Qiu, S.H., Chen, H., Luan, C.H., Carson, M., Tsao, J., Johnson, D., Lin, G., et al. (2002). Crystal structure of the cytoskeleton-associated protein glycine-rich (CAP-Gly) domain. J. Biol. Chem. *277*, 48596–48601.

Macias, M.J., Wiesner, S., and Sudol, M. (2002). WW and SH3 domains, two different scaffolds to recognize proline-rich ligands. FEBS Lett. *513*, 30–37.

Makris, C., Godfrey, V.L., Krahn-Senftleben, G., Takahashi, T., Roberts, J.L., Schwarz, T., Feng, L., Johnson, R.S., and Karin, M. (2000). Female mice heterozygous for IKK gamma/NEMO deficiencies develop a dermatopathy similar to the human X-linked disorder incontinentia pigmenti. Mol. Cell *5*, 969–979.

Makris, C., Roberts, J.L., and Karin, M. (2002). The carboxyl-terminal region of IκB kinase γ (IKKγ) is required for full IKK activation. Mol. Cell. Biol. *22*, 6573–6581.

McWhirter, S.M., Pullen, S.S., Holton, J.M., Crute, J.J., Kehry, M.R., and Alber, T. (1999). Crystrallographic analysis of CD40 recognition and signaling by human TRAF2. Proc. Natl. Acad. Sci. USA *96*, 8408–8413.

Morris, G.M., Goodsell, D.S., Halliday, R.S., Huey, R., Hart, W.E., Belew, R.K., and Olson, A.J. (1998). Automated docking using a Lamarckian genetic algorithm and and empirical binding free energy function. J. Comp. Chem. *19*, 1639–1662.

Ni, C.Z., Welsh, K., Leo, E., Chiou, C.K., Wu, H., Reed, J.C., and Ely, K.R. (2000). Molecular basis for CD40 signaling mediated by TRAF3. Proc. Natl. Acad. Sci. USA *97*, 10395–10399.

Park, Y.C., Burkitt, V., Villa, A.R., Tong, L., and Wu, H. (1999). Structural basis for self-association and receptor recognition of human TRAF2. Nature *398*, 533–538.

Pierre, P., Pepperkok, R., and Kreis, T.E. (1994). Molecular characterization of two functional domains of CLIP-170 in vivo. J. Cell Sci. *107*, 1909–1920.

Powers, R., Garrett, D.S., March, C.J., Frieden, E.A., Gronenborn, A.M., and Clore, G.M. (1993). The high-resolution, three-dimensional solution structure of human Interleukin-4 determined by multidimensional heteronuclear magnetic resonance spectroscopy. Biochemistry *32*, 6744–6762.

Prehoda, K.E., Lee, D.J., and Lim, W.A. (1999). Structure of the enabled/VASP homology 1 domain-peptide complex: a key component in the spatial control of actin assembly. Cell *97*, 471–480.

Radcliffe, P.A., and Toda, T. (2000). Characterisation of fission yeast alp11 mutants defines three functional domains within tubulin-folding cofactor B. Mol. Gen. Genet. *263*, 752–760.

Riehemann, K., and Sorg, C. (1993). Sequence homologies between four cytoskeleton-associated proteins. Trends Biochem. Sci. *18*, 82–83.

Rothwarf, D.M., Zandi, E., Natoli, G., and Karin, M. (1998). IKKγ is an essential regulatory subunit of the IκB kinase complex. Nature *395*, 297–300.

Rudolph, D., Yeh, W.C., Wakeham, A., Rudolph, B., Nallainathan, D., Potter, J., Elia, A.J., and Mak, T.W. (2000). Severe liver degeneration and lack of NF-kappaB activation in NEMO/IKKgamma-deficient mice. Genes Dev. *14*, 854–862.

Scheel, J., Pierre, P., Rickard, J.E., Diamantopoulos, G.S., Valetti, C., van der Goot, F.G., Haner, M., Aebi, U., and Kreis, T.E. (1999). Purification and analysis of authentic CLIP-170 and recombinant fragments. J. Biol. Chem. *274*, 25883–25891.

Schmidt-Supprian, M., Bloch, W., Courtois, G., Addicks, K., Israel, A., Rajewsky, K., and Pasparakis, M. (2000). NEMO/IKK gamma-deficient mice model incontinentia pigmenti. Mol. Cell *5*, 981–992.

Shi, C.S., and Kehrl, J.H. (2003). Tumor necrosis factor (TNF)-induced germinal center kinase-related (GCKR) and stress-activated protein kinase (SAPK) activation depends upon the E2/E3 complex Ubc13-Uev1A/TNF receptor-associated factor 2 (TRAF2). J. Biol. Chem. *278*, 15429–15434.

Smahi, A., Courtois, G., Vabres, P., Yamaoka, S., Heuertz, S., Munnich, A., Israel, A., Heiss, N.S., Klauck, S.M., Kioschis, P., et al. (2000). Genomic rearrangement in NEMO impairs NF-kappaB activation and is a cause of incontinentia pigmenti. The International Incontinentia Pigmenti (IP) Consortium. Nature *405*, 466–472.

Takahashi, M., Rapley, E., Biggs, P.J., Lakhani, S.R., Cooke, D., Hansen, J., Blair, E., Hofmann, B., Siebert, R., Turner, G., et al. (2000). Linkage and LOH studies in 19 cylindromatosis families show no evidence of genetic heterogeneity and refine the CYLD locus on chromosome 16q12-q13. Hum. Genet. *106*, 58–65.

Tang, E.D., Wang, C.Y., Xiong, Y., and Guan, K.L. (2003). A role for NF-kappaB essential modifier/IkappaB kinase-gamma (NEMO/IKKgamma) ubiquitination in the activation of the IkappaB kinase complex by tumor necrosis factor-alpha. J. Biol. Chem. *278*, 37297–37305.

Thomson, S.A., Rasmussen, S.A., Zhang, J., and Wallace, M.R. (1999). A new hereditary cylindromatosis family associated with CYLD1 on chromosome 16. Hum. Genet. *105*, 171–173.

Trompouki, E., Hatzivassiliou, E., Tsichritzis, T., Farmer, H., Ashworth, A., and Mosialos, G. (2003). CYLD is a deubiquitinating enzyme that negatively regulates NF-κB activation by TNFR family members. Nature *424*, 793–796.

Uren, A.G., and Vaux, D.L. (1996). TRAF proteins and meprins share a conserved domain. Trends Biochem. Sci. *21*, 244–245.

Wang, C., Deng, L., Hong, M., Akkaraju, G.R., Inoue, J., and Chen, Z.J. (2001). TAK1 is a ubiquitin-dependent kinase of MKK and IKK. Nature *412*, 346–351.

Yamaoka, S., Courtois, G., Bessia, C., Whiteside, S.T., Weil, R., Agou, F., Kirk, H.E., Kay, R.J., and Israel, A. (1998). Complementation cloning of NEMO, a component of the IκB kinase complex essential for NF-κB activation. Cell *93*, 1231–1240.

Ye, H., Park, Y.C., Kreishman, M., Kieff, E., and Wu, H. (1999). The structure basis for the recognition of diverse receptor sequences by TRAF2. Mol. Cell *4*, 321–330.

Zhou, H., Wertz, I., O'Rourke, K., Ultsch, M., Seshagiri, S., Eby, M., Xiao, W., and Dixit, V.M. (2004). Bcl10 activates the NF-kappaB pathway through ubiquitination of NEMO. Nature *427*, 167–171.

Accession Numbers

Coordinates have been deposited in the Protein Data Bank under the code number 1IXD.